ARTICLE
Journal of Cellular Biochemistry 114:1124–1134 (2013)

Journal of Cellular Biochemistry

Interplay of Reactive Oxygen Species, Intracellular Ca^{2+} and Mitochondrial Homeostasis in the Apoptosis of Prostate Cancer Cells by Deoxypodophyllotoxin

Kwang-Youn Kim,[1] Hyo-Jin Cho,[2] Sun-Nyoung Yu,[1] Sang-Hun Kim,[1] Hak-Sun Yu,[3] Yeong-Min Park,[1] Nooshin Mirkheshti,[4] So Young Kim,[4] Chung Seog Song,[4] Bandana Chatterjee,[4,5*] and Soon-Cheol Ahn[1,4,6**]

[1]*Department of Microbiology and Immunology, Pusan National University School of Medicine, Yangsan 626-870, Republic of Korea*

[2]*Brain Disease Research Center, Ajou University School of Medicine, Suwon 443-749, Republic of Korea*

[3]*Department of Parasitology, Pusan National University School of Medicine, Yangsan 626-870, Republic of Korea*

[4]*Department of Molecular Medicine and Institute of Biotechnology, The University of Texas Health Science Center at San Antonio, San Antonio, Texas 78245*

[5]*South Texas Veterans Health Care System, San Antonio, Texas 78229*

[6]*Medical Research Institute, Pusan National University, Yangsan 626-870, Republic of Korea*

ABSTRACT

The limited treatment option for recurrent prostate cancer and the eventual resistance to conventional chemotherapy drugs has fueled continued interest in finding new anti-neoplastic agents of natural product origin. We previously reported anti-proliferative activity of deoxypodophyllotoxin (DPT) on human prostate cancer cells. Using the PC-3 cell model of human prostate cancer, the present study reveals that DPT induced apoptosis via a caspase-3-dependent pathway that is activated due to dysregulated mitochondrial function. DPT-treated cells showed accumulation of the reactive oxygen species (ROS), intracellular Ca_i^{2+} surge, increased mitochondrial membrane potential (MMP, $\Delta\Psi_m$), Bax protein translocation to mitochondria and cytochrome *c* release to the cytoplasm. This resulted in caspase-3 activation, which in turn induced apoptosis. The antioxidant *N*-acetylcysteine (NAC) reduced ROS accumulation, MMP and Ca_i^{2+} surge, on the other hand the Ca^{2+} chelator BAPTA inhibited the Ca_i^{2+} overload and MMP without affecting the increase of ROS, indicating that the generation of ROS occurred prior to Ca^{2+} flux. This suggested that both ROS and Ca_i^{2+} signaling play roles in the increased MMP via Ca_i^{2+}-dependent and/or -independent mechanisms, since $\Delta\Psi_m$ elevation was reversed by NAC and BAPTA. This study provides the first evidence for the involvement of both ROS- and Ca_i^{2+}-activated signals in the disruption of mitochondrial homeostasis and the precedence of ROS production over the failure of Ca^{2+} flux homeostasis. J. Cell. Biochem. 114: 1124–1134, 2013.

KEY WORDS: DEOXYPODOPHYLLOTOXIN (DPT); APOPTOSIS; MITOCHONDRIAL MEMBRANE POTENTIAL (MMP); REACTIVE OXYGEN SPECIES (ROS); Ca^{2+} OVERLOAD

Conflict of interest: none.

Kwang-Youn Kim and Hyo-Jin Cho contributed equally to this work.

Grant sponsor: National Research Foundation of Korea (NRF); Grant number: 2012R1A1A2022587; Grant sponsor: US Department of Veterans Affairs 1I01BX000280.

*Correspondence to: Bandana Chatterjee, Department of Molecular Medicine, University of Texas Health Science Center at San Antonio, 15355 Lambda Drive, San Antonio, TX 78245. E-mail: chatterjee@uthscsa.edu

**Correspondence to: Soon-Cheol Ahn, Department of Microbiology and Immunology, Pusan National University School of Medicine, Yangsan 626-870, Republic of Korea. E-mail: ahnsc@pusan.ac.kr

Manuscript Received: 18 July 2012; Manuscript Accepted: 5 November 2012

Accepted manuscript online in Wiley Online Library (wileyonlinelibrary.com): 28 November 2012

DOI 10.1002/jcb.24455 • © 2012 Wiley Periodicals, Inc.

The lignan deoxypodophyllotoxin (DPT) is the natural constituent of a number of medicinal herb plants that is known to exert anti-proliferative effects and apoptosis on various cancer cell lines [Jin et al., 2011]. The anti-inflammatory property of this phytochemical further underscores its chemopreventive potential in cancer therapy, given that inflammation is recognized as having a crucial involvement in cancer etiology [De Marzo et al., 2007]. Inhibition of intracellular tubulin polymerization and induction of cell cycle arrest by DPT have been extensively reported. For example, HeLa uterine cancer cells accumulate at the G_2/M phase [Yong et al., 2009; Shin et al., 2010] and A549 lung cancer cells were arrested in the G_1 phase upon treatment with DPT. Synthetic derivatives of DPT were more potent in inhibiting cancer cell proliferation than the parent molecule [Jin et al., 2011]. The molecular machinery driving the death activity of these agents against cancer cells is not known.

Prostate cancer is a frequently diagnosed disease and is one of the leading causes of cancer deaths in men, especially in the United States and other industrialized nations. Pharmacologic inhibition of the androgen receptor (AR) pathway by depletion of circulating androgen and by anti-AR drugs is a standard-of-care treatment, which induces apoptosis in androgen-dependent prostate cancer cells and brings the disease to remission. However, the re-emergent cancer, which occurs in many patients, inevitably progresses to therapy resistance following response to conventional chemotherapy for a limited period. Finding new treatment options for therapy-resistant prostate cancer has been an overarching challenge [Yap et al., 2011]. Markedly reduced proliferation of the androgen-dependent LNCaP and androgen-independent PC-3 prostate cancer cells in response to DPT treatment was previously reported [Jiang et al., 2007; Cho et al., 2009]. A rigorous assessment of the therapeutic potential of DPT in prostate cancer requires mechanistic insights into the DPT-mediated inhibition of the cancer cell proliferation.

Some studies have reported that cancer chemopreventive agents induce apoptosis in part through reactive oxygen species (ROS) generation and disruption of redox homeostasis [Ling et al., 2003]. ROS are not only byproducts of mitochondrial respiration but also key signaling molecules that regulate mitochondrial dysfunction and apoptotic events [Liu et al., 2004]. As a secondary messenger, ROS has the ability to influence the mitochondrial function, mediate the elevation of intracellular Ca^{2+}, and lead to the activation of the caspase cascade [Paradies et al., 2002]. Pro-apoptotic signals such as ROS production can trigger the release of pro-apoptotic proteins from the mitochondria intermembrane space into the cytosol, such as, cytochrome *c*, caspase-9, apoptosis inducing factor, and Smac/DIABLO [Kroemer et al., 1998].

The mitochondrion-mediated intrinsic apoptosis, employing a cytochrome *c*/Apaf-1/caspase-9-dependent pathway, is the predominant route to the elimination of tumor cells by the majority of chemotherapeutic agents [Kaufmann and Earnshaw, 2000; Fulda and Debatin, 2006]. Loss of mitochondrial membrane potential (MMP, $\Delta\Psi_m$), resulting from the opening of the permeability transition pore, is an obligatory feature of the mitochondrial response to apoptotic stimuli that precedes DNA fragmentation and changes in the nuclear morphology [Mayer and Oberbauer, 2003]. Ca_i^{2+} overload in the mitochondrial matrix due to the dysregulation of the homeostasis in the intracellular Ca^{2+} flux, uncoupling of the electron transport chain and mitochondrial generation of ROS are some of the key events that lead to the permeability transition and loss of MMP.

Previously we isolated the bioactive compound DPT from the *Anthriscus sylvestris* root and demonstrated its anti-proliferative activity against human prostate cancer cells [Cho et al., 2009]. In the present study we have examined the mechanism that underlies prostate cancer cell death in the presence of DPT. Herein we report that DPT induces G_2/M cell cycle arrest and activates the intrinsic apoptotic pathway in the androgen-independent PC-3 prostate cancer cells. Also, we describe the role of ROS accumulation, intracellular Ca^{2+} surge and mitochondrial membrane hyperpolarization as part of the chain of events that led to apoptosis. Our results provide the first evidence that ROS production in response to DPT precedes the failure in Ca^{2+} flux homeostasis and that mitochondrial hyperpolarization is involved in the DPT-induced apoptotic loss of prostate cancer cells.

MATERIALS AND METHODS

REAGENTS AND ANTIBODIES

DPT used in this study was isolated by us from *A. sylvestris* roots and its structural identity was determined by nuclear magnetic resonance analysis as described previously [Cho et al., 2009]. The compound was confirmed to be >95% pure after high-performance liquid chromatography. 3-(4,5-Dimethyl-thiazol-2-yl)-2,5-diphenyl-tetrazolium bromide (MTT), *N*-acetylcysteine (NAC), 4′,6-diamidino-2-phenylindole dihydrochloride (DAPI), 3,3-dihexyloxacarbocyanine ($DiOC_6$), 2′-7′-dichlorodihydrofluorescein diacetate (DCFH-DA), 1,2-bis (2-aminophenoxy) ethane-N,N,N',N'-tetraacetic acid tetrakis (acetoxymethyl ester; BAPTA/AM), and Fluo-3/AM were purchased from Sigma Chemical Co. Annexin-V-Fluo Staining Kits and Caspase-3 Colorimetric Assay Kits were purchased from BD Biosciences and R&D Systems Inc., respectively. The ECL Western Kit was purchased from Amersham. Antibodies for Bax, Bcl-2, and poly (ADP-ribose) polymerase-1 (PARP-1) were purchased from Santa Cruz Biotechnology. Antibodies for cyclin B1, cdk-1, caspase-3, and cytochrome *c* were purchased from Cell Signaling.

CELL LINES AND CELL CULTURE

Prostate cancer cell lines, androgen-independent PC-3 cells, and androgen-dependent LNCaP cells, were obtained from the American Type Culture Collection (ATCC) and Korean Cell Line Bank (KCLB), respectively. These cells were maintained and cultured in Dulbecco's modified Eagle's medium (DMEM; WelGENE Inc.) and RPMI 1640 (WelGENE Inc.), respectively, supplemented with 10% fetal bovine serum (FBS; WelGENE Inc.), 100 units/ml of penicillin and 100 μg/ml of streptomycin (WelGENE Inc.). Cells were cultured in a humidified atmosphere with 5% CO_2 at 37°C.

CELL VIABILITY ASSAY

PC-3 cells and LNCaP cells were seeded in 48-well plates at a density of 1×10^4/well and treated with DPT of various concentrations at

different time points. After incubation, these cells were treated with 0.5 mg/ml of the MTT solution for further 4 h incubation and the precipitates were dissolved in dimethyl sulfoxide. A colorimetric analysis was performed at 570 nm with an ELISA reader (VERSA$_{max}$ microplate reader, Molecular Devices) [Jarrett et al., 2006]. Cell viability at a given time point was determined from the optical density of the treated cells relative to the untreated cells.

MORPHOLOGICAL CHANGES

PC-3 cells plated on chamber slides were either untreated or treated with 800 nM DPT for 24 h. Next, cells were fixed with 4% paraformaldehyde for 30 min, washed with phosphate buffered saline (PBS) twice and stained with DAPI solution (1 mg/ml) at 4°C for 15 min. Stained nuclei were visualized by laser scan confocal microscopy (FV-1000, Olympus) and the DAPI staining was used to analyze the apoptotic morphological change of cells.

CELL CYCLE ANALYSIS

PC-3 cells were plated in 6-well plates at a density of 1×10^5/well for 24 h after serum starvation overnight. The culture medium was refreshed with new medium and then the cells were treated with various concentrations of DPT for 24 h. And the cells were then fixed in 70% ethanol, washed with PBS twice and finally incubated in RNase A (200 μg/ml) at 37°C for 30 min. DNA content per cell was evaluated in flow cytometer (Becton Dickinson Co.) after staining cells with 1 mg/ml propidium iodide solution. Data collection and analysis of the cell cycle distribution were performed using Cell Quest and Modifit software (Becton Dickinson Co.).

ANNEXIN-V/PROPIDIUM IODIDE (PI) ASSAY

Apoptotic cells were detected by using an Annexin-V-Fluo staining kit. PC-3 cells, exposed to 8, 80, and 800 nM of DPT for 24 h in 6-well plates at a density of 1×10^4cells/well, were harvested, rinsed with PBS twice, mixed in 100 μl of 1× binding buffer and incubated with an Annexin-V/PI double staining solution at room temperature for 15 min. Stained cells were analyzed by flow cytometry. The percentage of apoptotic cells was calculated using Cell Quest software (Becton Dickinson Co.).

ASSESSMENT OF CASPASE-3 ACTIVITY

For detection of caspase-3 activation, a colorimetric assay kit (R&D Systems Inc.) was used according to the manufacturer's protocol.

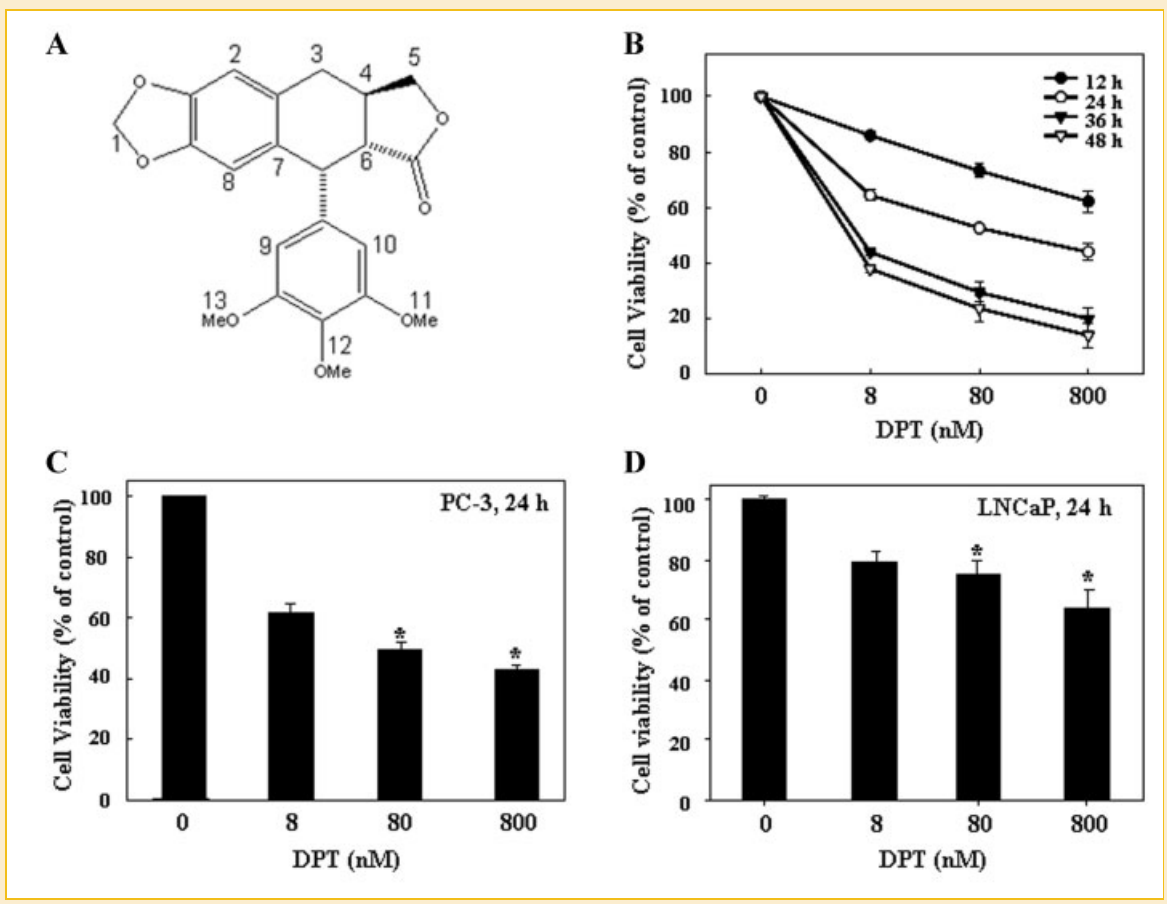

Fig. 1. Growth inhibition of prostate cancer cells by DPT. A: Chemical structure of DPT. B–D: Cell viability measurements. PC-3 cells (5×10^4 cells/ml) were treated with various concentrations of DPT (8, 80, and 800 nM) at different time points (12, 24, 36, and 48 h) (B), or at 24 h (C) and LNCaP cells (D) were at 24 h. Cell viability was determined by a 3-(4,5-dimethyl-thiazol-2-yl)-2,5-diphenyl-tetrazolium bromide (MTT) assay. Data are mean ± SD (n = 3 in each group). *$P < 0.05$ versus control group.

Equal amounts of protein (220 μg) were resuspended in reaction buffer containing substrate (Ac-DEVD-pNA) and then incubated at 37°C for 4 h in the dark. The absorbance of the released pNA was measured at 405 nm using an ELISA reader.

MEASUREMENT OF INTRACELLULAR REACTIVE OXYGEN SPECIES (ROS)

Intracellular ROS was measured using the DCFH-DA fluorescent dye. PC-3 cells were treated with 80 nM DPT for indicated times and then incubated with 10 μM DCFH-DA at 37°C for 30 min and then washed twice with PBS. For each experiment, the cells were analyzed for DCFH-DA fluorescence by flow cytometry.

ANALYSIS OF INTRACELLULAR Ca^{2+} CONCENTRATION

Intracellular Ca_i^{2+} levels were determined using the Ca^{2+}-sensitive fluorescence dye Fluo-3/AM. After exposure to DPT at various concentrations for 8 and 24 h, cells were centrifuged and washed twice with PBS and then incubated with 5 μM Fluo-3/AM at 37°C for 30 min. Then the cells were washed and subjected to flow cytometry.

MEASUREMENT OF MITOCHONDRIAL MEMBRANE POTENTIAL (MMP)

MMPs ($\Delta\Psi_m$) were determined from the retention of the dye $DiOC_6$, which is a mitochondrial membrane potential sensitive dye. PC-3 cells were collected at 8 and 24 h after treatment with an 8, 80, and 800 nM of DPT and washed twice with PBS, and incubated with 100 nM $DiOC_6$ at 37°C for 30 min. The washed cells were analyzed by flow cytometry for $DiOC_6$ fluorescence.

WESTERN BLOTTING

Cell extracts were prepared by incubating the cells in lysis buffer [150 mM NaCl, 10 mM Tris (pH 7.4), 5 mM EDTA (pH 8.0), 1% Triton X-100, 1 mM PMSF, 20 mg/ml aprotinin, 50 μg/ml leupeptin, 1 mM benzidine, and 1 mg/ml pepstatin]. Forty micrograms of proteins were electrophoretically separated using sodium dodecyl sulfate-polyacrylamide gel electrophoresis (SDS–PAGE) on a 12–15% gel and transferred to a polyvinylidenefluoride (PVDF) membrane (Amersham). After blocking with TBS-T buffer [20 mM Tris (pH 7.4), 150 mM NaCl, 0.1% Tween 20] containing 5% skim milk, the membranes were incubated with primary and secondary antibodies. The membranes were then washed with TBS-T buffer and visualized with ECL Western blotting detection reagents (Amersham). The density of each band was determined with a fluorescence scanner (LAS 3000, Fuji Film) and analyzed with Multi Gauge V3.0 software.

MITOCHONDRIAL AND CYTOSOLIC FRACTIONS

Release of pro-apoptotic factors from the mitochondria to the cytosol was detected by Western blotting using a Qproteome™ Mitochondria isolation Kit (Qiagen) according to the manufacturer's instructions. Western blotting was carried out according to the protocol described in the previous section.

STATISTICAL ANALYSIS

Experiments were repeated at least three times with consistent results. Unless otherwise stated, data are expressed as the mean ± SD. ANOVA was used to compare the experimental groups with the control, whereas comparisons among multiple groups were performed using a Tukey's multiple comparison test. Results were statistically significant at $P < 0.05$.

RESULTS

SUSCEPTIBILITY OF PROSTATE CANCER CELLS TO DEOXYPODOPHYLLOTOXIN (DPT)

DPT, a polycyclic aromatic molecule (Fig. 1A), reduced the viability of PC-3 cells in a dose- and time-dependent manner (Fig. 1B). Comparison of the proliferation rates of the LNCaP and PC-3 cells in the presence of DPT revealed a higher susceptibility of the latter cell type (Fig. 1C vs. D). For PC-3 cells, 24 h incubation with DPT at 80 and 800 nM caused ~50% and 60% reduction in cell viability, respectively, whereas the viability of LNCaP cells was reduced by ~25% and 40%, respectively, under the same conditions. Thus, DPT

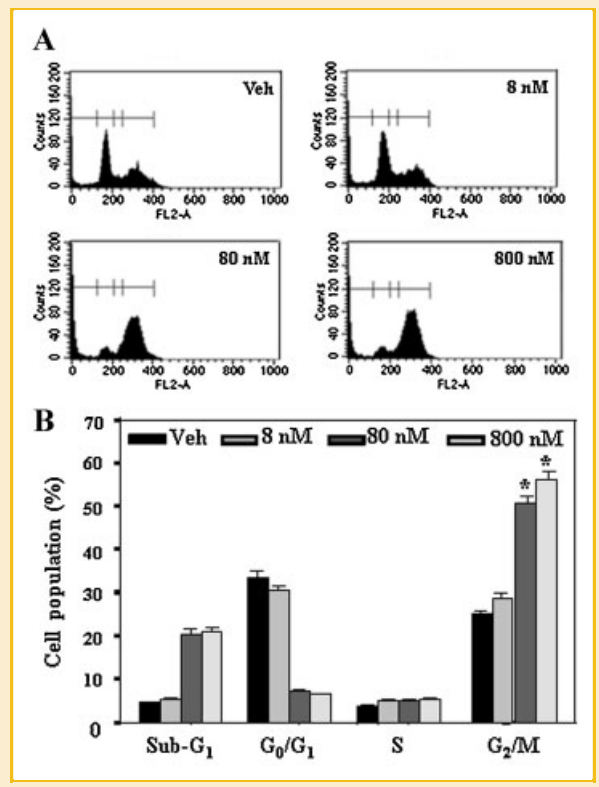

Fig. 2. Effect of DPT on PC-3 cell cycle progression. A: G_2/M cell cycle arrest, revealed from flow cytometry. B: Quantification of cell populations at various phases of cell cycle. After treatment with DPT for 24 h, the cells were fixed with ice-cold 70% ethanol at −20°C and then stained with propidium iodide (1 mg/ml), followed by flow cytometery. Data are presented as mean ± SD ($n = 3$, each group). *$P < 0.05$ versus control group.

may be more efficient in ablating the highly aggressive and chemotherapy-resistant PC-3 cancer cells than the hormone-responsive, poorly metastatic LNCaP cells. We focused on the PC-3 cell model to examine the molecular events associated with the DPT-induced cell loss.

G_2/M PHASE CELL CYCLE ARREST BY DPT

Cell cycle progression and the expression of a number of cell cycle-related proteins in PC-3 cells were examined in the presence and absence of DPT. PC-3 cells treated with 8, 80, and 800 nM of DPT for 24 were analyzed by flow cytometry using propidium iodide (PI) staining. A representative cell cycle profile is shown in Fig. 2A. The cell population in the G_2/M phase increased from 26.11% in control, untreated cells to 30.34% and 52.02% when the cells were treated with 8 and 80 nM of DPT, respectively (Fig. 2B). These results show that DPT induces G_2/M arrest of PC-3 cells, similar to what was reported for HeLa cells, which were prevented by DPT from cell cycle progression due to a blockade at G_2/M [Yong et al., 2009; Shin et al., 2010]. The levels of cyclin B1 and cdk1 did not change in the cells treated with DPT for 24 h, although at 48 h, the treated cells showed reduced levels of these proteins (data not shown).

APOPTOSIS OF DPT-TREATED PC-3 CELLS

Staining of DPT-treated PC-3 cells with DAPI revealed a high percentage of non-adherent cells and a clear indication of nuclear condensation, which is a hallmark feature of apoptotic cells. Reduction in the cell volume was also observed. This contrasted the vehicle-treated control cells, which appeared normal with round nuclei and all of these cells adhered to the culture plate (Fig. 3A). Annexin-V-FITC staining of the cells provided further evidence for DPT-induced apoptosis (Fig. 3B). Thus, flow cytometry analysis shows that after treatment with DPT for 24 h, the early and late

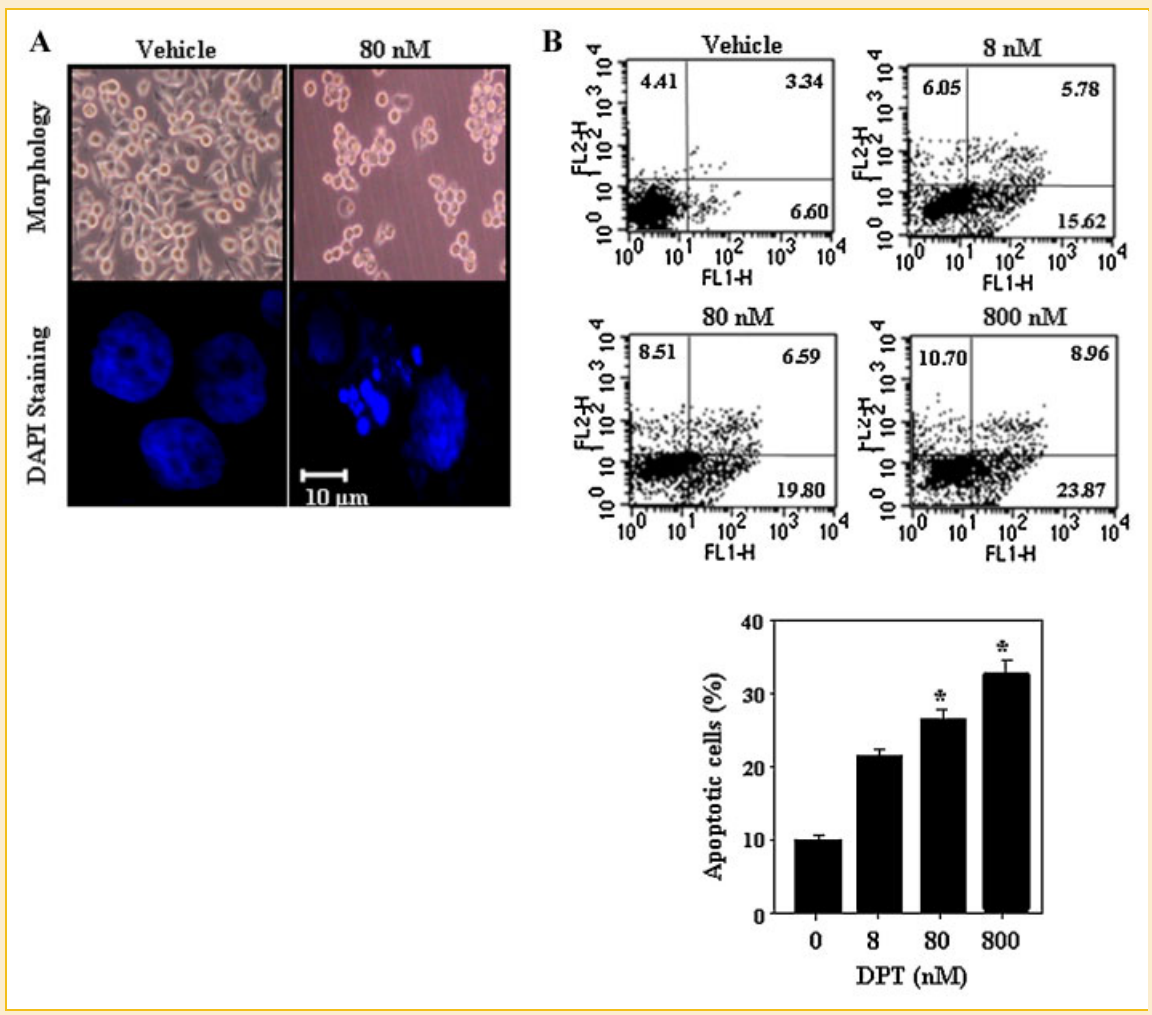

Fig. 3. DPT-induced apoptosis in PC-3 cells. A: Cytomorphological changes. After treatment with DPT for 24 h, nuclear fragmentation was observed by light and laser scanning confocal microscopy. Magnification, 1,800×. B: Flow cytometric analysis. PC-3 cells were treated with various concentrations of DPT for 24 h and stained with Annexin-V/propidium iodide (PI). The dual parameter dot plots combining Annexin-V-fluorescein isothiocyanate (FITC) and PI fluorescence show the viable cell population in the lower left quadrant (Annexin-V^-PI^-), the apoptotic cells in the lower right quadrant (Annexin-V^+PI^-) together with the upper right quadrant (Annexin-V^+PI^+), and necrotic cells in the upper left quadrant (Annexin-V^-PI^+). Data are presented as mean ± SD (n = 3 in each group). $^*P < 0.05$ versus control group.

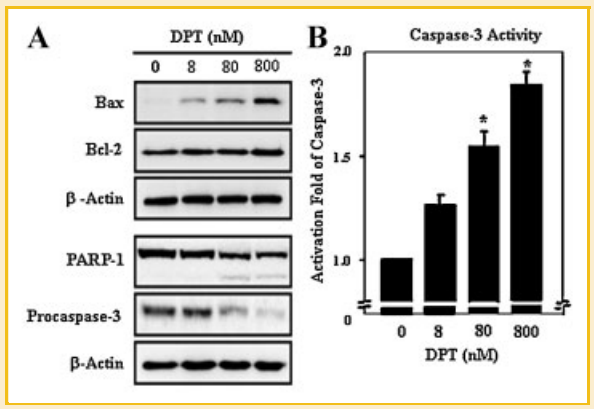

Fig. 4. Regulation of apoptosis-related protein levels in DPT-treated PC-3 cells. A: Immunoblots of Bax, Bcl-2, procaspase-3 and poly (ADP-ribose) polymerase (PARP-1) levels. Cells were exposed to 8, 80, and 800 nM of DPT for 24 h. B: Caspase-3 activity. The activity was determined by colorimetric assay using a specific substrate (Ac-DEVD-pNA). Data are presented as mean ± SD (n = 3 in each group). $^{*}P < 0.05$ versus control group.

apoptotic PC-3 cells increased from 9.79% in untreated cells to 21.40% and 26.39% at 8 and 80 nM, respectively (Fig. 3B). Apoptosis was further augmented when the DPT concentration increased to 800 nM. These results indicate that the DPT-induced morphological changes negatively affected the growth of PC-3 cells, which subsequently underwent apoptosis.

CHANGES IN THE PRO-APOPTOTIC AND ANTI-APOPTOTIC BCL-2 FAMILY PROTEINS AND ACTIVATION OF CASPASE-3

Induction of the PC-3 cell apoptosis in the presence of DPT prompted us to examine the expression dynamics of the apoptosis- and survival-related proteins in the Bcl-2 family and the conversion of the pro-caspase-3 zymogen to active caspase in the total cell lysate using Western blotting. The pro-apoptotic Bax protein level was induced by DPT after incubation for 24 h at as low as 8 nM concentration and the induction increased steadily with higher concentrations of DPT 80 and 800 nM, whereas the Bcl-2 anti-apoptotic protein did not show any significant change within the total cell lysate at any of the DPT concentrations (Fig. 4A, upper panels). In a coordinate and dose-dependent manner, DPT-mediated events led to the reduction of the pro-caspase-3 zymogen level, indicating the generation of caspase-3, which in turn caused cleavage of PARP-1, a well-characterized caspase-3 substrate (Fig. 4A, lower panels). Induction of the caspase-3 activity in DPT-treated PC-3 cells was further confirmed using a colorimetric assay for caspase-3 activity (Fig. 4B). These results establish a role of DPT in the induction of caspase-3-dependent

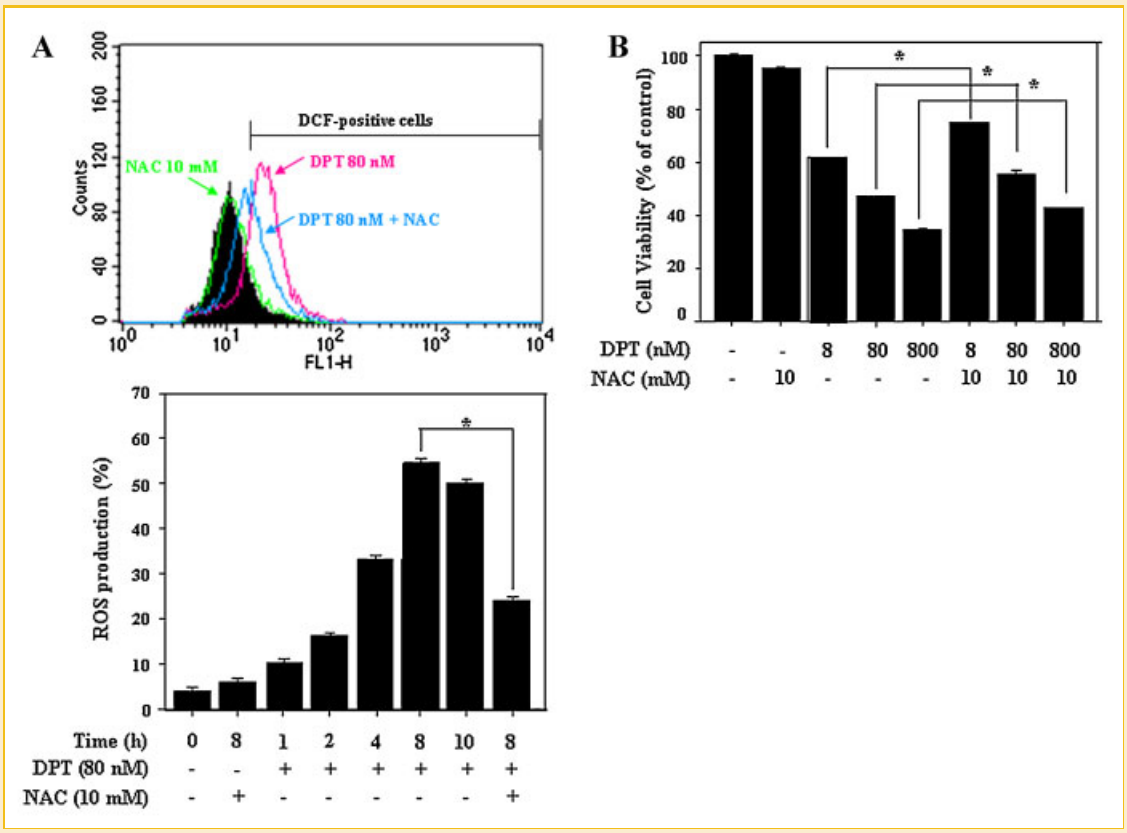

Fig. 5. ROS production in DPT-treated PC-3 cells. A: Intracellular ROS levels. Cells were treated with 80 nM DPT for the indicated times in the presence or absence of a prior 1 h incubation with 10 mM *N*-acetylcysteine (NAC). The dichlorodihydrofluorescein (DCF) fluorescence intensity in the cells was detected by flow cytometry. B: Cell viability determined by MTT assay. Cells were treated with 8, 80, and 800 nM DPT for 24 h in the presence or absence of prior 1 h incubation with 10 mM *N*-acetylcysteine (NAC). Data are mean ± SD (n = 3 in each group). $^{*}P < 0.05$ versus control group.

apoptosis in PC-3 cells that follows induction of the pro-apoptotic protein Bax.

ACCUMULATION OF REACTIVE OXYGEN SPECIES (ROS)

It has been reported that the ROS level in cells correlates with the induction of mitochondrial permeability dysfunctions, and cancer chemotherapy drugs mediate apoptosis in part by promoting ROS production in a variety of tumor cell types [Ouyang et al., 2002; Ling et al., 2003]. The intracellular ROS level, measured from the fluorescence intensity, increased within 1 h of exposure to 80 nM DPT and the highest level of ROS (55.17% from the basal level) was observed from the DPT exposure for 8 h (Fig. 5A, lower panel). ROS production was prevented when the cells were treated with the antioxidant *N*-acetylcysteine (NAC) for 1 h prior to DPT exposure (Fig. 5A, upper panel). In the presence of 10 mM of NAC, we observed 24.26% recovery of the number of DCF-positive PC-3 cells that were treated with 80 nM DPT for 8 h (Fig. 5A, lower panel). The viability of DPT-treated PC-3 cells also increased in the presence of NAC, showing an increase from 62.16% to 80.08% at 8 nM DPT and 51.40% to 61.21% after 24 h incubation of 80 nM DPT (Fig. 5B). However, the recovery of cell viability was not complete at any of the conditions that we examined. It is possible that a complete recovery requires a higher concentration of NAC, which we could not test since NAC by itself also exerted a cytotoxic effect on these cells. Nevertheless, the results in Figure 6 indicate that ROS production plays an important role in the DPT-induced apoptosis in PC-3 cells.

MITOCHONDRIAL MEMBRANE HYPERPOLARIZATION, BAX TRANSLOCATION AND CYTOCHROME *c* RELEASE

Flow cytometry analysis of $DiOC_6$ fluorescence dye stained cells was performed to assess mitochondrial membrane potential (MMP, $\Delta\psi_m$) before and after treatment with DPT for 24 h. After treatment with 80 nM DPT at 8 h, DPT induced unique mitochondrial

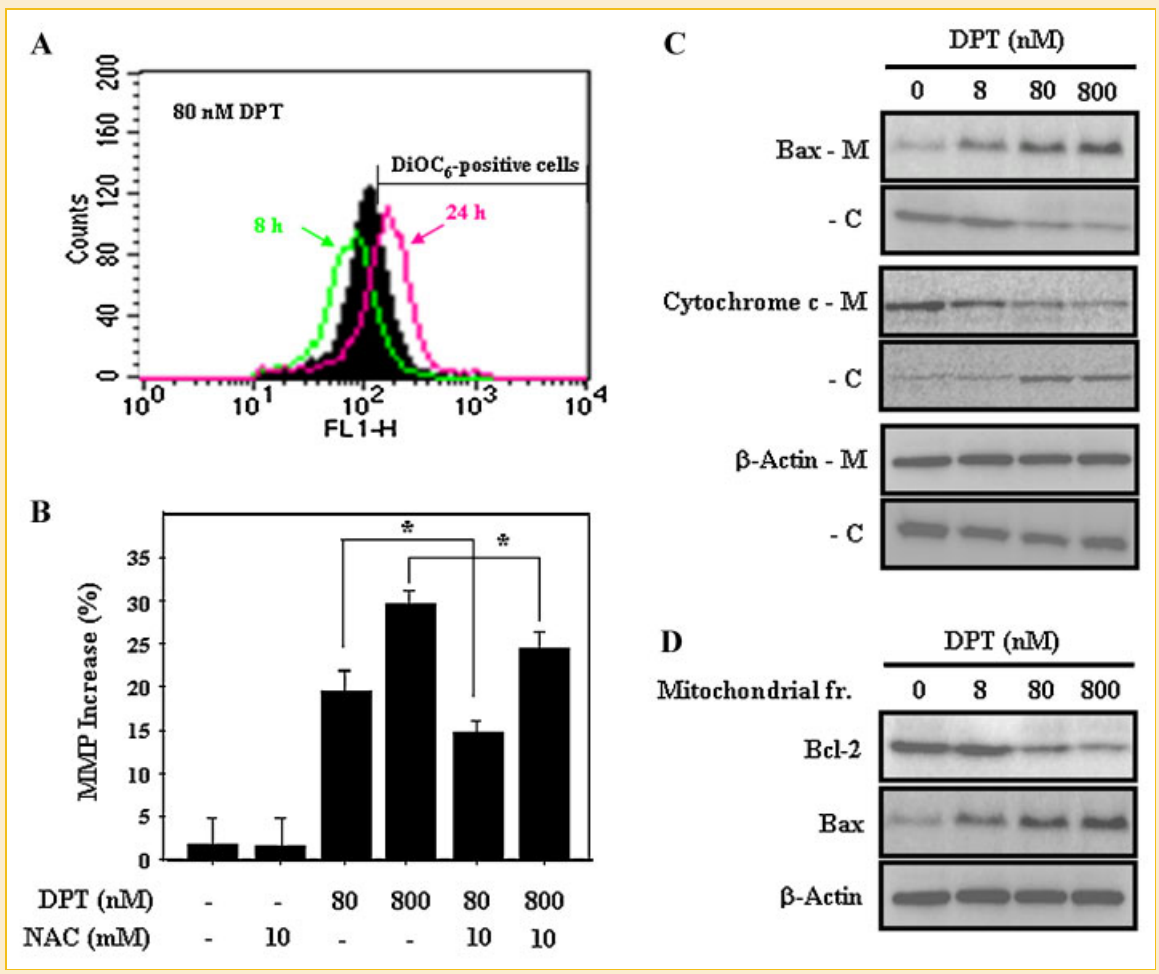

Fig. 6. Effects of DPT on mitochondrial membrane potential (MMP). A: Time course of MMP. PC-3 cells were treated with 80 nM DPT for indicated time. Changes in MMP ($\Delta\psi_m$) were determined from the shift in $DiOC_6$ fluorescence and analyzed by flow cytometry. B: Effect of NAC on MMP. PC-3 cells were treated with 80 nM DPT for 24 h in the presence or absence of prior 1 h incubation with 10 mM NAC. C: Mitochondrial (M) and cytoplasmic (C) levels of apoptosis-related proteins. D: Levels of Bax and Bcl-2 in the mitochondrial fraction. PC-3 cells were treated with 8, 80, and 800 nM DPT for 24 h. The levels of Bax and cytochrome *c* in the cytosol and mitochondrial fractions were determined by Western blotting. Data are mean ± SD (n = 3 in each group). $^*P < 0.05$ versus control group.

membrane depolarization (Fig. 6A). However, after longer treatment for 24 h, the depolarization peak was shifted to hyperpolarization in dose-dependent manner (Fig. 6A,B). The mitochondrial membrane hyperpolarization was partially prevented when the cells were pretreated with 10 mM NAC for 24 h (Fig. 6B). These data indicated that the MMP dysfunction occurred at the downstream of ROS production. Furthermore, the MMP dysfunction was linked to the translocation of Bax from the cytoplasm to the mitochondrion and mitochondrial cytochrome *c* release to the cytosol (Fig. 6C). Thus, in Western blot assay, the mitochondrial fraction of the treated cells showed progressively higher levels of Bax at increasing doses of DPT with a parallel reduction in the cytosolic Bax level (Fig. 6C). DPT also provoked elevation in the cytosolic level of cytochrome *c* along with its concomitantly reduced level in the mitochondria (Fig. 6C). In addition, the increased Bax level in the mitochondrial fraction of the treated cells was accompanied by a coordinated decrease in the anti-apoptotic survival protein Bcl-2 (Fig. 6D). These results indicate that DPT initiates a cascade of events that result in the redistribution of critical components of the caspase-3-dependent apoptotic pathway between the cytosol and mitochondria.

Ca_i^{2+} FLUX IN DPT-TREATED CELLS

Disruption of intracellular calcium homeostasis is one of the characteristic events associated with mitochondrial membrane disruption and apoptosis. We used Fluo-3/AM, a Ca^{2+}-sensitive fluorescence probe, to monitor changes in the intracellular Ca^{2+} level. The fluorescence emitted from 80 nM DPT treated cells was shifted to a higher intensity in time-dependent manner, indicating a DPT-induced surge in the intracellular Ca_i^{2+} concentration (Fig. 7A). But the Ca^{2+} chelator BAPTA/AM significantly reduced the Ca_i^{2+} surge (Fig. 7B). The rise in the Ca_i^{2+} concentration was partially blocked when the cells were pretreated with NAC and this blockade was statistically significant (Fig. 7C), indicating that the ROS production and the resulting oxidant stress are involved in the elevation of the Ca_i^{2+} level in the treated cells with 80 nM DPT.

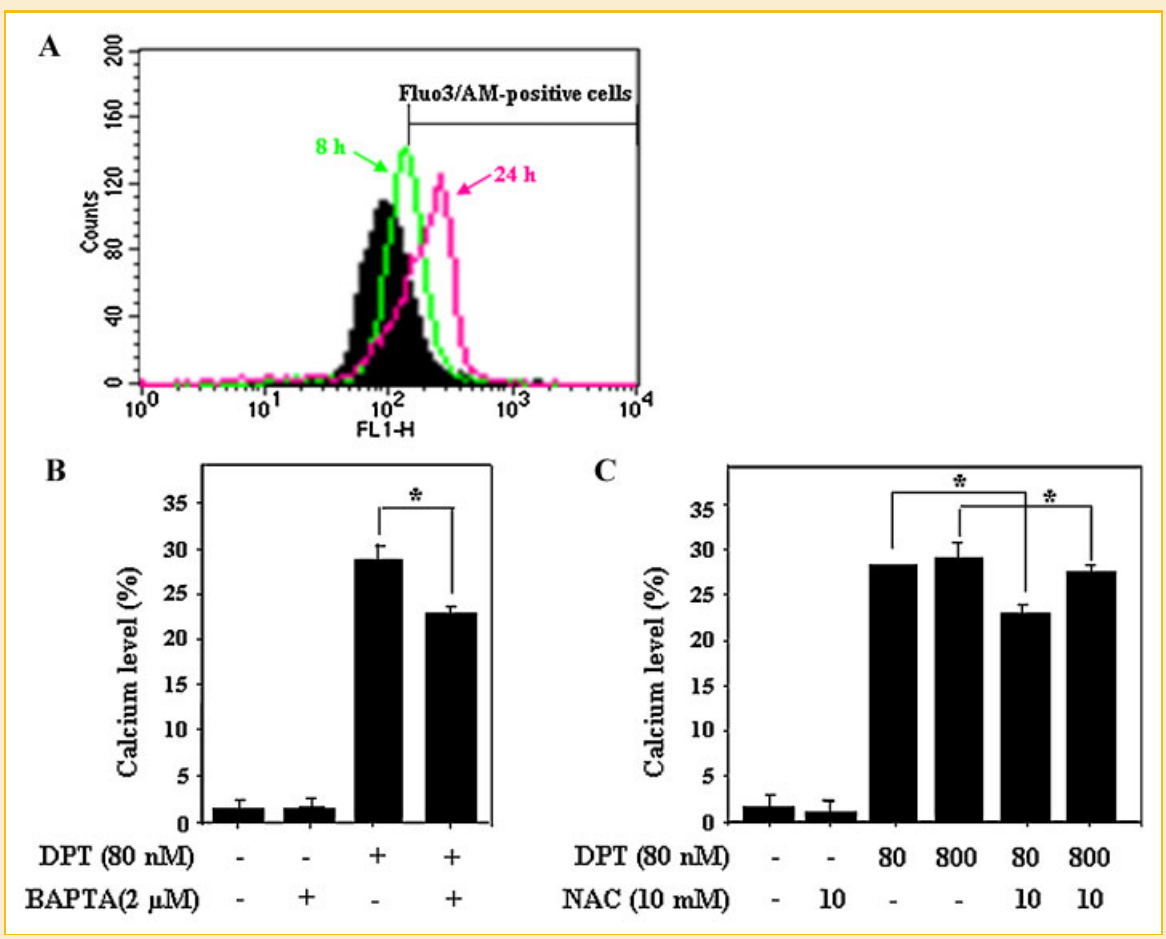

Fig. 7. Intracellular Ca_i^{2+} concentration in DPT-treated PC-3 cells. A: Intracellular Ca^{2+} flux. Cells were treated with 80 nM DPT for various times. B: Effect of BAPTA on Ca_i^{2+} level. Cells were treated with 80 nM DPT for 24 h in the presence or absence of prior 1 h incubation with 2 μM BAPTA. C: The effect of NAC on the Ca_i^{2+} level. Cells were treated with 80 and 800 nM DPT for 24 h in the presence or absence of prior 1 h incubation with 10 mM NAC. The Ca_i^{2+} concentration was determined by flow cytometry using Fluo-3/AM fluorescence. Data are mean ± SD (n = 3 in each group). $^*P < 0.05$ versus control group.

DEPENDENCE OF Ca_i^{2+} SURGE ON ROS PRODUCTION AND MMP AND CELL VIABILITY

By the pretreatment with BAPTA/AM, a cell-permeable Ca^{2+} chelator, ROS induction in the presence of DPT was not prevented (Fig. 8A) but the increased MMP by DPT was significantly attenuated (Fig. 8B). The hyperpolarization decreased by 4.75%, that is, from 19.49% to 14.74%. Inhibition of the Ca_i^{2+} surge by NAC (Fig. 7C) but continued ROS accumulation despite the chelation of Ca_i^{2+} (Fig. 8A). Also, after the pretreatment with BAPTA/AM, cell viability and apoptosis of PC-3 cells in the presence of DPT were significantly recovered (Fig. 8C,D), when taken together, led us to conclude that the ROS production in the treated cells precedes the release of intracellular Ca_i^{2+}. Furthermore, since both NAC and BAPTA/AM attenuated mitochondrial hyperpolarization (Figs. 6B and 8B), we conclude that both Ca_i^{2+} overload-dependent and -independent mechanisms are involved in the regulation of the mitochondrial dysfunction by the oxidant stress from ROS accumulation and by the Bcl-2 family from redistribution in mitochondria, respectively.

DISCUSSION

Deoxypodophyllotoxin (DPT), a natural product of several medicinal plants, potently inhibits prostate cancer cell proliferation and induces apoptosis. Our data show that the androgen-independent PC-3 human prostate cancer cells are more susceptible to DPT-mediated growth inhibition than the androgen-dependent LNCaP human prostate cancer cells. The present study was conducted to elucidate the molecular basis for the DPT-induced apoptosis in the PC-3 cell model. We show that DPT induced the following (1) cell cycle arrest at G_2/M; (2) intracellular reactive oxygen species (ROS) accumulation; (3) intracellular Ca_i^{2+} surge; (4) hyperpolarization of the mitochondrial membrane; (5) translocation of the pro-apoptotic Bcl-2 family member Bax to mitochondria along with reduction in the mitochondrial level of the anti-apoptotic protein Bcl-2 and hence, a decline in the mitochondrial ratio of Bcl-2 to Bax; (6) cytoplasmic release of cytochrome *c* from the mitochondrial intermembrane space; and (7) caspase-3 activation leading to PARP-1 cleavage and nuclear condensation that culminated in the apoptotic cell death (Fig. 9).

Previously we had reported that the antibiotic salinomycin induces apoptosis in several human prostate cancer cells, including PC-3 cells, by elevating the intracellular ROS level, which was accompanied by decreased MMP. Unlike DPT, salinomycin-treated PC-3 cells did not show any change in the intracellular Ca_i^{2+} concentration [Kim et al., 2011], indicating that disparate mechanisms are at play for cancer cell apoptosis by structurally unrelated natural products. We observed G_2/M arrest of DPT-treated PC-3 cells, similar to what was reported for HeLa cells [Shin et al., 2010]. DPT induced p53 expression in HeLa cells that resulted

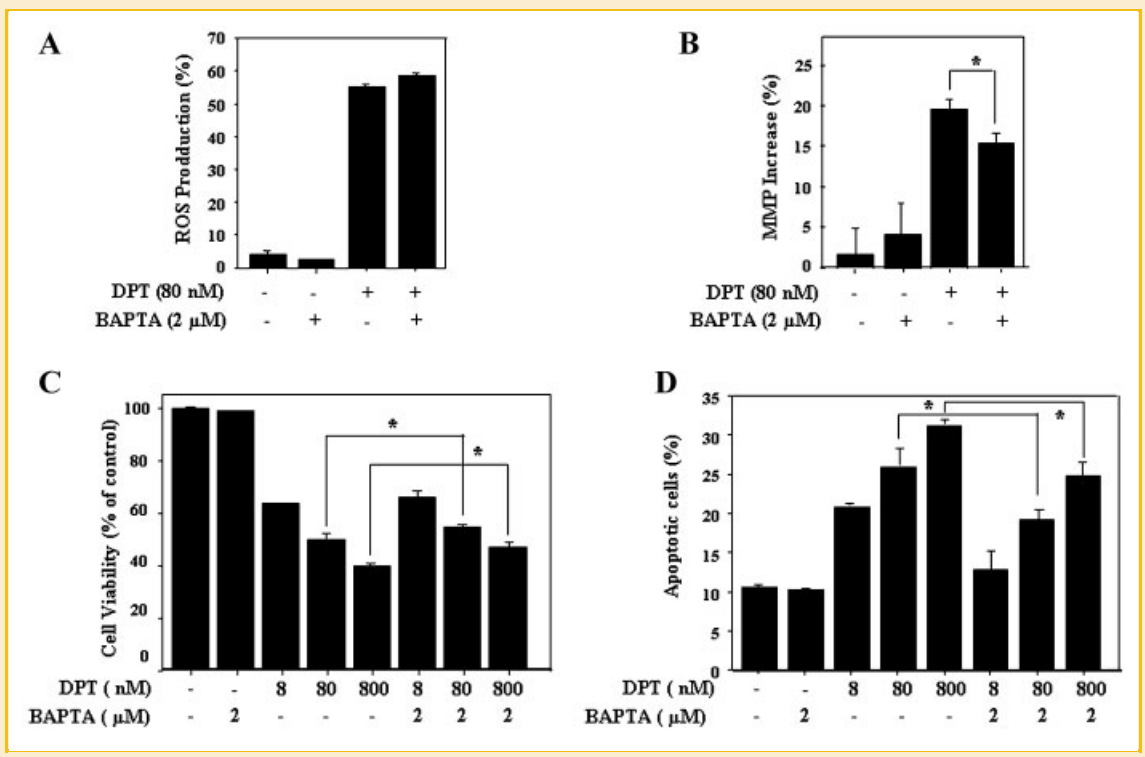

Fig. 8. Effect of BAPTA on ROS production, MMP and cell viability in PC-3 cells. A: ROS production. B: MMP measurement. C: Cell viability. D: Apoptotic cell death. For (A,B), PC-3 cells were treated with 80 nM DPT for 24 h in the presence or absence of prior 1 h incubation with 2 μM BAPTA. For (C,D), DPT treatment at indicated concentrations was for 24 h. Intensities of dichlorodihydrofluorescein and $DiOC_6$ and Annexin-V/PI fluorescence were detected by flow cytometry analysis, respectively. Data are mean ± SD (n = 3 in each group). $^*P < 0.05$ versus control.

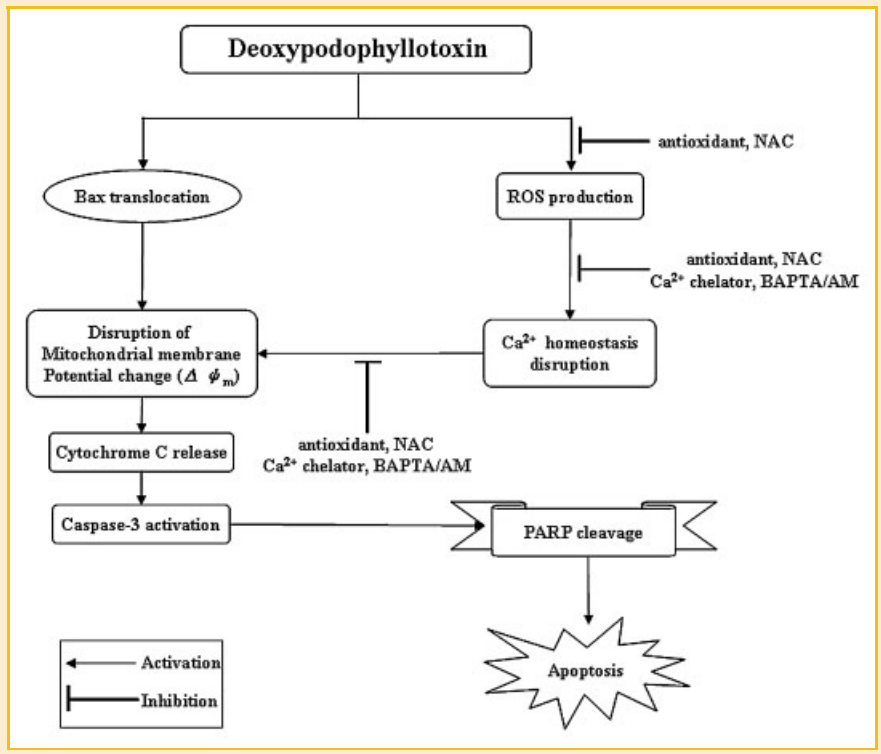

Fig. 9. An integrated depiction of the results from the current study that show the role of ROS and Ca_i^{2+} signaling in the DPT-induced disruption of mitochondrial homeostasis, caspase-3 activation and apoptosis in PC-3 prostate cancer cells.

in a p53-dependent DNA damage response, revealed from the activation of the DNA damage-sensing kinases such as ATM and Chk2 [Shin et al., 2010]. It will be important to determine whether PC-3 cell apoptosis by DPT also associates with a DNA damage response.

In a number of experimental models of apoptosis, hyperpolarization of the mitochondrial membrane has been detected as an early event, leading to induction of apoptosis [Li et al., 1999; Giovannini et al., 2002; Kim et al., 2003; Cao et al., 2007]. The events leading to mitochondrial hyperpolarization are not well-understood; it has been speculated that the cell type, cellular environment and duration of apoptotic stimuli may dictate the underlying mechanism for hyperpolarization [Kim et al., 2003]. Opposite to published reports, our results show a biphasic phenomenon that a drop in MMP occurred as an early event within 8 h post-DPT treatment and MMP was shifted to increased $\Delta\psi_m$ at 24 h and furthermore even at 72 h post-DPT treatment the hyperpolarization was sustained (data not shown). In case of the methyl protodioscin-induced apoptosis of K562 leukemia cells, elevated $\Delta\psi_m$ was detected for up to 60 h post-treatment and thereafter, loss of MMP ensued [Kim et al., 2003]. Time course analysis utilizing early as well as late time points and utilization of a synchronized cell population will be needed to thoroughly address this apparent anomaly.

We conclude that ROS is produced prior to the endoplasmic reticulum stress and that Ca^{2+} release is under ROS regulation, since the antioxidant *N*-acetylcysteine (NAC) reduced both intracellular ROS accumulation and Ca^{2+} overload, whereas the Ca^{2+} chelator BAPTA interfered with only the Ca_i^{2+} surge without affecting ROS accumulation. Hyperpolarization of the mitochondrial membrane potential (MMP) was observed in PC-3 cells at the 24 h time point post DPT treatment, and the rise of MMP was attenuated by NAC as well as BAPTA. This suggests that both ROS and the Ca_i^{2+} overload contributed to the increased MMP, and the mitochondrial dysfunction by the oxidant stress from ROS accumulation may involve Ca_i^{2+} overload-dependent as well as -independent mechanisms.

In conclusion, the present study provides new insights into the role of ROS- and Ca_i^{2+}-activated signals in the DPT-induced disruption of mitochondrial homeostasis in prostate cancer cells. Additional insights into the DPT-induced cross talks among multiple signaling networks that are involved in the disruption of mitochondrial homeostasis and induction of apoptosis in cancer cell lines, in primary tumor cells and in animal models will help assess the potential utility of DPT and its derivatives in the management of therapy-resistant advanced prostate cancer.

ACKNOWLEDGMENTS

This research was supported by Basic Science Research Program through the National Research Foundation of Korea (NRF) funded by the Ministry of Education, Science and Technology (2012R1A1A2022587) and by a Merit Review grant (1I01BX000280) from the US Department of Veterans Affairs. B.C. is a VA Senior Research Career Scientist.

REFERENCES

Cao J, Liu Y, Jia L, Zhou HM, Kong Y, Yang G, Jiang LP, Li QJ, Zhong LF. 2007. Curcumin induces apoptosis through mitochondrial hyperpolarization and mtDNA damage in human hepatoma G2 cells. Free Radic Biol Med 43:968–975.

Cho HJ, Yu SN, Kim KY, Sohn JH, Oh H, Ahn SC. 2009. Screening and purification of an anti-prostate cancer compound, deoxypodophyllotoxin, from *Anthriscus sylvestris* Hoffm, J. Life Sci 19:9–14.

De Marzo AM, Platz EA, Sutcliffe S, Xu J, Gronberg H, Drake CG, Nakai Y, Isaacs WB, Nelson WG. 2007. Inflammation in prostate carcinogenesis. Nat Rev Cancer 7:256–269.

Fulda S, Debatin KM. 2006. Extrinsic versus intrinsic apoptosis pathways in anticancer chemotherapy. Oncogene 25:4798–4811.

Giovannini C, Matarrese P, Scazzocchio B, Sanchez M, Masella R, Malorni W. 2002. Mitochondria hyperpolarization is an early event in oxidized low-density lipoprotein-induced apoptosis in Caco-2 intestinal cells. FEBS Lett 523:200–206.

Jarrett SG, Albon J, Boulton M. 2006. The contribution of DNA repair and antioxidants in determining cell type-specific resistance to oxidative stress. Free Radic Res 40:1155–1165.

Jiang RW, Zhou JR, Hon PM, Li SL, Zhou Y, Li LL, Ye WC, Xu HX, Shaw PC, But PP. 2007. Lignans from Dysosma versipellis with inhibitory effects on prostate cancer cell lines. J Nat Prod 70:283–286.

Jin Y, Liu J, Huang WT, Chen SW, Hui L. 2011. Synthesis and biological evaluation of derivatives of 4-deoxypodophyllotoxin as antitumor agents. Eur J Med Chem 46:4056–4061.

Kaufmann SH, Earnshaw WC. 2000. Induction of apoptosis by cancer chemotherapy. Exp Cell Res 256:42–49.

Kim JM, Bae HR, Park BS, Lee JM, Ahn HB, Rho JH, Yoo KW, Park WC, Rho SH, Yoon HS, Yoo YH. 2003. Early mitochondrial hyperpolarization and intracellular alkalinization in lactacystin-induced apoptosis of retinal pigment epithelial cells. J Pharmacol Exp Ther 305:474–481.

Kim KY, Yu SN, Lee SY, Chun SS, Choi YL, Park YM, Song CS, Chatterjee B, Ahn SC. 2011. Salinomycin-induced apoptosis of human prostate cancer cells due to accumulated reactive oxygen species and mitochondrial membrane depolarization. Biochem Biophys Res Commun 413:80–86.

Kroemer G, Dallaporta B, Resche-Rigon M. 1998. The mitochondrial death/life regulator in apoptosis and necrosis. Annu Rev Physiol 60:619–642.

Li PF, Dietz R, von Harsdorf R. 1999. p53 regulates mitochondrial membrane potential through reactive oxygen species and induces cytochrome *c*-independent apoptosis blocked by Bcl-2. EMBO J 18:6027–6036.

Ling YH, Liebes L, Zou Y, Perez-Soler R. 2003. Reactive oxygen species generation and mitochondrial dysfunction in the apoptotic response to Bortezomib, a novel proteasome inhibitor, in human H460 non-small cell lung cancer cells. J Biol Chem 278:33714–33723.

Liu MJ, Wang Z, Li HX, Wu RC, Liu YZ, Wu QY. 2004. Mitochondrial dysfunction as an early event in the process of apoptosis induced by woodfordin I in human leukemia K562 cells. Toxicol Appl Pharmacol 194:141–155.

Mayer B, Oberbauer R. 2003. Mitochondrial regulation of apoptosis. News Physiol Sci 18:89–94.

Ouyang YB, Carriedo SG, Giffard RG. 2002. Effect of Bcl-x(L) overexpression on reactive oxygen species, intracellular calcium, and mitochondrial membrane potential following injury in astrocytes. Free Radic Biol Med 33:544–551.

Paradies G, Petrosillo G, Pistolese M, Ruggiero FM. 2002. Reactive oxygen species affect mitochondrial electron transport complex I activity through oxidative cardiolipin damage. Gene 286:135–141.

Shin SY, Yong Y, Kim CG, Lee YH, Lim Y. 2010. Deoxypodophyllotoxin induces G2/M cell cycle arrest and apoptosis in HeLa cells. Cancer Lett 287:231–239.

Yap TA, Zivi A, Omlin A, de Bono JS. 2011. The changing therapeutic landscape of castration-resistant prostate cancer. Nat Rev Clin Oncol 8:597–610.

Yong Y, Shin SY, Lee YH, Lim Y. 2009. Antitumor activity of deoxypodophyllotoxin isolated from Anthriscus sylvestris: Induction of G2/M cell cycle arrest and caspase-dependent apoptosis. Bioorg Med Chem Lett 19:4367–4371.